Scattering of Electromagnetic Waves by a Material Half-Space with a Time-Varying Conductivity

Fady A. Harfoush, *Member, IEEE*, and Allen Taflove, *Fellow, IEEE*

Abstract—**This paper analyzes for the first time electromagnetic wave penetration and scattering interactions for a material half-space having sinusoidally time-varying conductivity. Two limiting cases are considered. The first assumes that the material conductivity is almost a constant with a small temporal perturbation. The problem is accordingly attacked with first-order perturbation methods. The second exploits a large dimensionless parameter and yields an asymptotic expansion of the field inside a highly conducting material undergoing sinusoidal time variation. Illustrative examples are given which agree well with numerically obtained finite-difference time-domain (FDTD) results.**

I. Introduction

ELECTROMAGNETIC wave propagation and scattering interactions with media having time-varying parameters has been extensively studied. However, most published work considers only time-varying permittivity or permeability [1]–[4], and not time-varying conductivity. Yet, time-varying volumetric conductivity resulting from a nuclear burst, atmospheric fluctuations, or other environmental changes can markedly affect wave propagation. Further, time-varying surface conductivity can affect the fields that are radiated and scattered from objects. These phenomena can be exploited for engineering benefit if appropriate understanding could be developed.

Scattering problems involving media with temporally and/or spatially varying permittivity have been analyzed using Mathieu functions [1] and Floquet representations [5], [6]. Although a general Floquet representation is possible for a medium with time-varying conductivity, the resulting recursive relation describing the modal amplitudes is very complicated and difficult to solve. Here, it is no longer possible to obtain a Mathieu type differential equation, regardless of the assumed conductivity variation.

In this paper, we consider the scattering and propagation problem for a material half-space whose conductivity is a periodic function of time alone. The emphasis is on the mathematical tools utilized to obtain an approximate solution. A physical interpretation of the final results is also presented. To verify our analytical results, comparison is made whenever possible, against purely numerical results generated by a finite-difference time-domain (FDTD) method [7]. Finally, and to further verify our results, the analysis is checked in the limit of constant conductivity both analytically and numerically. The incident radiation is a step-modulated time-harmonic plane wave of frequency ω_i. To enable an approximate mathematical result, we analyze two different cases and limits. In Case 1, the conductivity is given by $\sigma(t) = \sigma_0(1 + \epsilon f(t))$, where σ_0 is a reference conductivity, ϵ is the amplitude of the modulation, and $f(t)$ is a periodic function of time with period ω_σ. We develop an asymptotic approximation of the fields in the limit as $\epsilon \to 0$ with σ_0 and ω_σ held fixed. This results in simple expressions that agree well with FDTD results.

In Case 2, the conductivity is given by $\sigma(t) = \sigma_0/[1 + \epsilon f(t)]$, but now ϵ and ω_σ are fixed while $\sigma_0 \to \infty$. Here, the material half-space is highly conductive with a substantial time variation. We develop two asymptotic schemes for analyzing this limit. To obtain the scattered field, we apply a boundary layer analysis for the material region close to the interface. To obtain the fields within the material, we apply (with some modifications) a method developed by Lewis [8] to study the short-term behavior of parabolic equations. In the present context, we assume that the fields within the material are proportional to the product of a slowly changing amplitude and a rapidly decaying exponential. The determination of the exponent and the amplitude parallels classical geometrical optics in as much as a nonlinear first-order partial differential eikonal equation determines the exponent and a "transport" equation determines the amplitude. We obtain space-time rays, which carry the wave into the half-space. This representation breaks down near the interface. However, this nonuniformity can be removed by matching the "ray" solution to the boundary layer solution mentioned above [12].

The remainder of the paper is organized as follows. Section II defines the problem and introduces the dimensionless quantities of interest. Section III analyzes Case 1, the half-space with slightly modulated conductivity. Section IV presents the two analyses for Case 2 and determines the scattered field in the large-conductivity limit. Section V describes the matching of the asymptotic solutions of Case 2. Finally, Section VI summarizes the various results and conclusions.

Manuscript received May 9, 1989; revised September 6, 1990. This work was supported in part by National Science Foundation Grant ASC-8811273 and by the Office of Naval Research under Contract N00014-88-K-0475.

F. A. Harfoush is with the Fermi National Accelerator Laboratory, MS 345, P.O. Box 500, Batavia, IL 60510.

A. Taflove is with the Department of Electrical Engineering and Computer Science, Technological Institute, Northwestern University, Evanston, IL 60208.

IEEE Log Number 9100556.

0018-926X/91/0700-0898$01.00

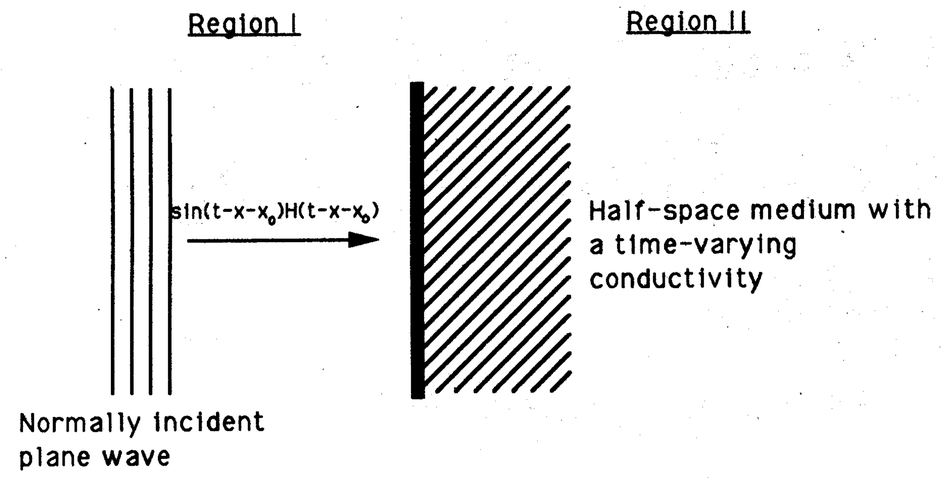

Fig. 1. Plane wave incident on a half-space media with a time-varying conductivity.

II. Problem Definition

A plane electromagnetic wave traveling in the $+x$ direction is normally incident on a material half-space with a time-varying conductivity $\sigma(t) = \sigma_0 f(\nu t)$ (see Fig. 1). The partial differential equation describing the normalized wave electric field in the medium, $\Omega \equiv E_z / E_0$, is given by

$$\Omega_{xx} = \Omega_{tt} + \alpha(\Omega f)_t, \qquad x > 0, \tag{1}$$

where x and t are dimensionless variables defined by $x \equiv kx'$, $t \equiv \omega_i t'$; k and ω_i are, respectively, the free space wavenumber and the incident wave frequency, and where α and ν are dimensionless parameters defined by $\alpha \equiv \sigma_0 / \epsilon_0 \omega_i$, $\nu \equiv \omega_\sigma / \omega_i$. Here, the primes denote the dimensioned quantities and E_0 is the amplitude of the incident wave. Parameter α is denoted as the material dissipation factor.

We assume that the total field in free space, $x < 0$, is given by

$$\vec{E} = E_0\{U(t-x)H(t-x-x_0) + U^{sc}(x,t)\}\vec{z}, \tag{2}$$

identifying H as the Heaviside step function, $U^{inc} = U(t-x)H(t-x-x_0)$ as the incident field, and U^{sc} as the scattered field. Throughout this paper, we assume a sinusoidal dependence of the incident wave,

$$U(t-x) = \sin(t-x-x_0). \tag{3}$$

The required continuity of the tangential E and H fields at the medium interface and the form of (2) gives the following boundary condition for Ω at $x = 0$:

$$\Omega_t(0,t) - \Omega_x(0,t) = 2\frac{\partial U^{inc}(t)}{\partial t} \equiv g(t). \tag{4}$$

In addition to (4), Ω must be an outgoing wave at $x = \infty$ and satisfy the initial conditions

$$\Omega(x > 0, 0) = \Omega_t(x > 0, 0) = 0. \tag{5}$$

These initial conditions are due to the Heaviside step function present in the incident field, and imply that the wavefront is at $x = -x_0$ at time $t = 0$.

The initial boundary value problem (1)–(5) has no closed-form solution for any time-periodic conductivity. We shall, therefore, develop asymptotic approximations to the fields for the two separate cases described in the introduction, and validate these approximations using the purely numerical FDTD method.

III. Case 1: Perturbation Analysis for the Low-Amplitude Conductivity Variation

In this section, we consider half-space conductivity variations of the form

$$\sigma(t) = \sigma_0(1 + \epsilon \sin(\nu t + \psi)) \tag{6}$$

where $\epsilon \ll 1$ and ψ is a phase shift. We first assume that Ω is given inside the medium by the regular perturbation expansion

$$\Omega(x,t) = \Omega_0 + \epsilon\Omega_1 + \epsilon^2\Omega_2 + ,\cdots, \quad x > 0. \tag{7}$$

Inserting this expansion into (1), (4), and (5) and equating to zero the coefficients of the powers of ϵ, we obtain an infinite set of differential equations, boundary conditions, and initial data which sequentially determine the Ω_n. The zero-order problem is given by

$$\Omega_{0xx} = \Omega_{0tt} + \alpha\Omega_{0t}, \qquad x > 0 \tag{8}$$

$$\Omega_{0t} - \Omega_{0x} = 2H(t-x_0)\cos(t-x_0), \qquad x = 0 \tag{9}$$

$$\Omega_0 = \Omega_{0t} = 0, \qquad t = 0. \tag{10}$$

The complete solution of this problem can be obtained by transform methods because the conductivity bias σ_0 is constant. The transient solution is given by the integral

$$-\frac{2\alpha}{\pi}\int_0^1 \frac{e^{-\alpha v t}\sqrt{v - v^2}}{1 + \alpha^2 v^2}\, dv \tag{11}$$

where the interval [0, 1] defines a branch cut in the complex plane of integration. The "steady-state" solution as $t \to \infty$ is given by

$$\Omega_0 = \frac{2}{\left[(1-\gamma_r)^2 + \gamma_i^2\right]^{1/2}} \cos(t + \gamma_i x + \varphi) \tag{12}$$

where $\gamma = \gamma_r + j\gamma_i \equiv \sqrt{j\alpha - 1}$ is the complex propagation constant. The phase shift φ is introduced by the complex nature of γ.

The first-order problem for Ω_1 is given by

$$\Omega_{1xx} = \Omega_{1tt} + \alpha\Omega_{1t} + \alpha \sin \nu t\Omega_{0t} + \nu\alpha \cos \nu t\Omega_0 \tag{13}$$

$$\Omega_{1t} - \Omega_{1x} = 0, \qquad x = 0 \tag{14}$$

$$\Omega_1 = \Omega_{1t} = 0, \qquad t = 0 \tag{15}$$

which now has a forced term due to Ω_0 and the presence of the modulated conductivity. Again, this problem can be solved completely by transform techniques. The steady-state result can be shown to be

$$\Omega_1 = \frac{\alpha}{2}\operatorname{Re}\left\{\left[k_1 e^{\gamma x} + Ae^{\delta x}\right]e^{j(\nu+1)t} + \left[k_2 e^{\gamma x} + Be^{\beta x}\right]e^{j(1-\nu)t}\right\} \tag{16}$$

where

$$k_1 = \frac{\alpha\tau}{2}\frac{\nu + 1}{(\gamma^2 - \delta^2)} \tag{17}$$

$$A = \frac{\left[j(\nu+1) - \gamma\right]}{\gamma^2 - \delta^2}\frac{k_1}{\left[\delta - j(\nu+1)\right]} \tag{18}$$

$$k_2 = \frac{\alpha\tau}{2}\,\frac{\nu - 1}{(\gamma^2 - \beta^2)} \tag{19}$$

$$B = \frac{[j(1-\nu) - \gamma]}{\gamma^2 - \beta^2}\,\frac{k_2}{[\beta - j(1-\nu)]} \tag{20}$$

and

$$\delta = \sqrt{j\alpha(\nu+1) - (\nu+1)^2},$$

$$\beta = \sqrt{j\alpha(1-\nu) - (1-\nu)^2},$$

and Re denotes the real part of a complex number. The new variable τ is the transmission coefficient due to a constant bias σ_0, and is equal to $2/[1 + \sqrt{j\alpha - 1}\,]$.

To find the scattered field, we assume again a solution of the form

$$U^{sc} = U_0^{sc} + \epsilon U_1^{sc} + \epsilon^2 U_2^{sc} + \cdots . \tag{21}$$

From the continuity of the field at the boundary and the fact that each U_n^{sc} term satisfies a homogeneous wave equation in free space, the zero-order steady-state scattered field can be shown to be

$$U_0^{sc} = \text{Re}\,\rho e^{j(t+x)} \tag{22}$$

where ρ is the reflection coefficient due to the constant bias σ_0,

$$\rho = \frac{1 - \sqrt{j\alpha - 1}}{1 + \sqrt{j\alpha + 1}}\,. \tag{23}$$

The first-order steady-state scattered field can be shown to equal

$$U_1^{sc} = \frac{\alpha}{2}\,\text{Re}\left\{[k_1 + A]\,e^{j(\nu+1)(x+t)} + [k_2 + B]\,e^{j(1-\nu)(x+t)}\right\} \tag{24}$$

where k_1, A, k_2, B are defined above.

We now compare the total scattered field amplitude obtained (to order ϵ^2) from (21)–(24) to purely numerical results obtained using FDTD. Fig. 2 shows the variation of the scattered-field amplitude at the illumination frequency versus the initial phase shift (ψ) between the incident wave and the time-varying conductivity for $\sigma_0 = 1$, $\epsilon = 0.2$, and $\nu = 2$ and 3. The first-order approximation is seen to agree very well with the FDTD results. We also see that for $\nu = 2$, i.e., $\omega_\sigma = 2\omega_i$, there exists an amplitude dependence on the initial phase shift. (The same behavior will also be observed in Section IV with the asymptotic result.) For $\nu = 3$ and other values of $\nu \neq 2$ (not shown here), there is no amplitude dependence on phase shift. This is found to be true even for values quite close to 2, as for example $\nu = 2.1$. This strongly suggests an interference effect that occurs only for conductivity variations at twice the incident frequency. Such an effect at $\nu = 2$ is plausible since the scattered field at the boundary involve a zero-order term like $\cos(t + \psi)$ and a first-order term like $\cos((\nu - 1)t)$. For $\nu = 2$ these two terms can then add up to result in a reflected field amplitude at the illumination frequency that varies with the phase ψ and is 2π periodic.

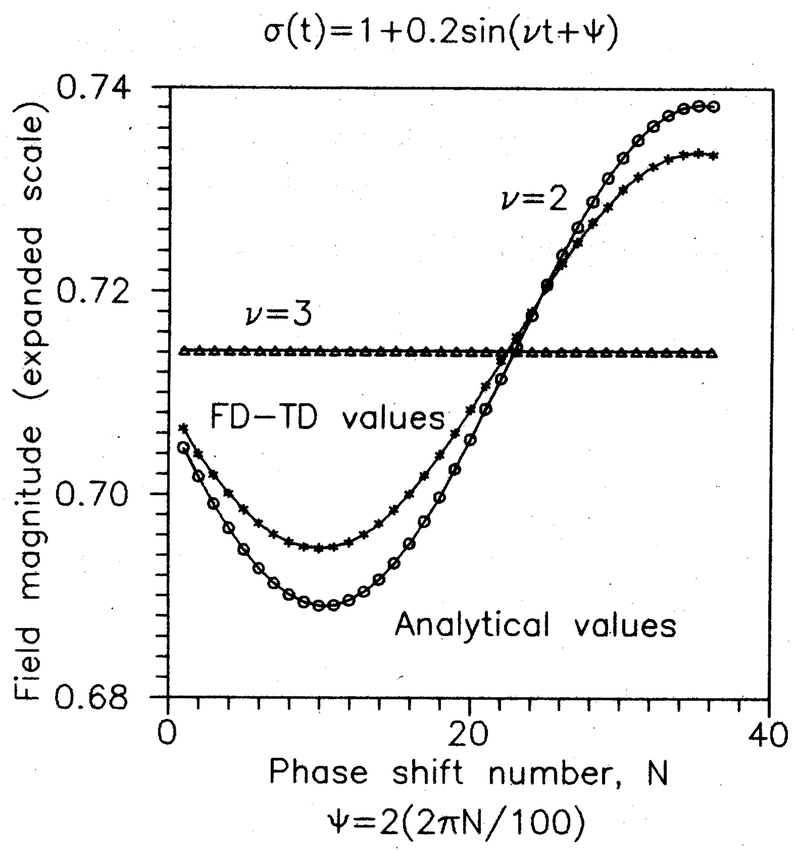

Fig. 2. Reflected field amplitude at the illumination frequency versus the initial phase shift ϕ as obtained both by FDTD and the first-order perturbation analysis.

IV. Case 2: Boundary Layer Analysis for the Time-Variable Highly Conducting Half-Space

In this section, we consider half-space conductivity variations of the form $\sigma(t) = \sigma_0/1 + \epsilon\sin(\nu t + \psi)$ in the limit of large conductivity; i.e,. $\sigma_0 \to \infty$ with ν and ϵ fixed. If we wish only to determine the scattered field, the required information can be obtained by analysis of the structure of the half-space field within the first few skin depths. In terms of the dimensionless distance x, this corresponds to $x \simeq 1/\sqrt{\alpha}$. The analysis of this "boundary-layer" is carried out in Section IV-A.

If, on the other hand, we require detailed knowledge of the field penetrating the time varying conductor, a different type of field expansion is needed. In Section IV-B, an asymptotic approximation is constructed which is strictly valid for $x \gg 1/\sqrt{\alpha}$ and $t \gg 1/\alpha$. This approximation becomes invalid near $x = 0$ for all time, where the boundary layer expansion of Section IV-A becomes valid. However, both representations are valid in a small region, and this permits the expansions to be matched.

Finally, we observe that both field expansions become invalid near $x = t = 0$. In Section V, we will perform a local analysis and show that it matches into the other representations.

A. The Boundary Layer Near $x = 0$

We begin by introducing the stretched (or boundary layer) variable $\bar{x} = \sqrt{\alpha}\,x$ (which we take to be of order unity) into (1) and (4). We obtain

$$\Omega_{\bar{x}\bar{x}} = (\Omega f)_t + \frac{1}{\alpha}\,\Omega_{tt}, \qquad \bar{x} > 0 \tag{25}$$

$$\Omega_t - \sqrt{\alpha}\,\Omega_{\bar{x}} = g(t), \qquad \text{at } \bar{x} = 0. \tag{26}$$

For large α, we assume that Ω has the asymptotic representation

$$\Omega = \sum_{m=1}^{m=\infty} \frac{1}{\sqrt{\alpha^m}}\,\Omega_m(\bar{x}, t). \tag{27}$$

Substituting this ansatz in (25) and (26) and equating to zero the coefficients of the powers of $\sqrt{\alpha}$, we obtain an infinite set of boundary value problems which sequentially determine the Ω_m. Since we are only interested in a leading-order term, we restrict our attention to Ω_1. It satisfies

$$\Omega_{1\bar{x}\bar{x}} = (\Omega_1 f)_t \tag{28}$$

$$\Omega_{1\bar{x}} = g(t) \tag{29}$$

$$\Omega_1(\bar{x}, 0) = \Omega_{1t}(\bar{x}, 0) = 0 \tag{30}$$

where (30) follows from (5) and (27). By performing the following change of variables

$$\Omega_1(\bar{x}, t) f(t) = V_1(\bar{x}, t) \tag{31}$$

$$\xi = \int_0^t \frac{dt}{f(t)} \tag{32}$$

we transform (28)–(30) to

$$V_{1\bar{x}\bar{x}} = V_{1\xi}, \qquad \bar{x} > 0, \xi > 0 \tag{33}$$

$$V_{1\bar{x}} = h(\xi), \qquad \bar{x} = 0, \xi > 0 \tag{34}$$

$$V_1 = 0, \qquad \text{at } \xi = 0 \tag{35}$$

where $h(\xi) \equiv g(t(\xi)) f(t(\xi))$ and $t(\xi)$ is given by the inverse of (32). This is a diffusion equation and we have accordingly only prescribed one homogeneous piece of initial data, (35). The solution to (33) can not satisfy the second condition in (30), namely $V_{1\psi} = 0$ at $\psi = 0$. This gives rise to a nonuniformity in (27) which we resolve in Section V. It is therefore seen that for large α the equation takes the form of a diffusion equation. This is in accordance with the general approach to solve Maxwell's equations with large α. Here the displacement current is neglected with respect to the conduction current. This leads to a diffusion equation in electric field. The ambiguity as to how can we match a propagating wave solution in region I to a diffusing (nonpropagating) wave solution in region II will become clear later. As mentioned in the beginning of Section IV this solution is valid only in a region of order $1/\alpha$ and breaks down at $x = t = 0$.

The solution of (33) is readily found by transform or Green's function techniques [9]

$$V_1(\bar{x}, \xi) = \frac{-1}{\sqrt{\pi}} \int_0^{\xi} \frac{h(\xi')}{\sqrt{\xi - \xi'}} e^{-\frac{\bar{x}^2}{4(\xi - \xi')}} d\xi'. \tag{36}$$

When $\bar{x} \gg 1$, so that we are beginning to penetrate several skin depths into the material, (36) reduces to

$$V_1(\bar{x}, \xi) \simeq \frac{\xi^{3/2}}{\bar{x}^2} e^{-\frac{\bar{x}2}{4\xi}} \tag{37}$$

as we can show by integrating (36) by parts. Thus, for a fixed t (and hence ξ), the field decays as a Gaussian distribution. The value of V_1 at $\bar{x} = 0$ is given by

$$V_1(0, \xi) = \frac{-1}{\sqrt{\pi}} \int_0^{\xi} \frac{h(\xi')}{\sqrt{\xi - \xi'}} d\xi' \tag{38}$$

and is needed to determine the scattered field. Its evaluation can be done, in principle, by numerical quadrature. However, if ν is an integer, or the reciprocal of an integer (so that ω_σ and ω_i are harmonically related frequencies), we can proceed further with our analysis. In this case $h(\xi)$ is a periodic function of ξ and can be written as

$$h(\xi') = \sum_{-\infty}^{\infty} c_n e^{j\frac{2\pi n \xi'}{\zeta}} \tag{39}$$

where the coefficients c_n are defined by

$$c_n = \frac{2}{\zeta} \int_0^{\zeta} h(\xi) e^{-j\frac{2\pi n \xi}{\zeta}} d\xi. \tag{40}$$

The parameter ζ is a period of $h(\xi)$. By introducing t as the variable of integration via (32), (40) becomes

$$c_n = \frac{2}{T} \int_0^{T} \cos(t) e^{-j\frac{2\pi n \xi(t)}{T}} dt \tag{41}$$

where T is the period of h as a function of t.

We now introduce (39) into (38) and interchange the order of integration and summation. We obtain after a change of variables in the integral

$$V_1(0, \xi) = \sum_{n=\infty}^{\infty} c_n e^{2\pi n j \frac{\xi}{\zeta}} F\left(2n\pi \frac{\xi}{\zeta}\right) \sqrt{\frac{2\zeta}{n\pi}} \tag{42}$$

where F is the Fresnel integral defined here by

$$F(s) = \int_0^{\sqrt{s}} e^{-jp^2} dp. \tag{43}$$

Since the conductivity function $f(t)$ is positive, $\xi(t)$ monotonically increases with t, a fact that we have taken implicitly in the statement of (33). Thus, as $t \to \infty$ we have $\xi \to \infty$. Now, in this limit, (42) simplifies to

$$V_1(0, t) = 4 \sum_{n=1}^{\infty} \sqrt{\frac{\zeta}{2n\pi}} c_n \sin\left(\frac{2\pi n \xi}{\zeta} + \frac{\pi}{4}\right) \tag{44}$$

because

$$F(\infty) = \frac{\sqrt{\pi}}{2} e^{-j\frac{\pi}{4}}. \tag{45}$$

It should be noted here that at $x = 0$ and $t \to \infty$ the solution form for V_1 given by (44) is oscillating in time. This oscillation is necessary to match the propagating solution to the diffusive equation at the boundary $x = 0$ between the two regions. Finally, we combine (44), (27), (28), and (2) with the fact that $\vec{E}$ is continuous at $x = \bar{x} = 0$ to obtain

$$U^{sc}(0, t) = -\sin t + \frac{1}{\sqrt{\alpha}} \frac{V_1(0, \xi(t))}{f(t)} + O(1/\alpha) \tag{46}$$

where $O(1/\alpha)$ denotes the remaining terms in (27). Since the scattered field satisfies the wave equation for $x < 0$, it must be a function of the argument $x + t$. Thus, the scattered field is given for large time and for $x < 0$ by (46) with t replaced by $(t + x)$.

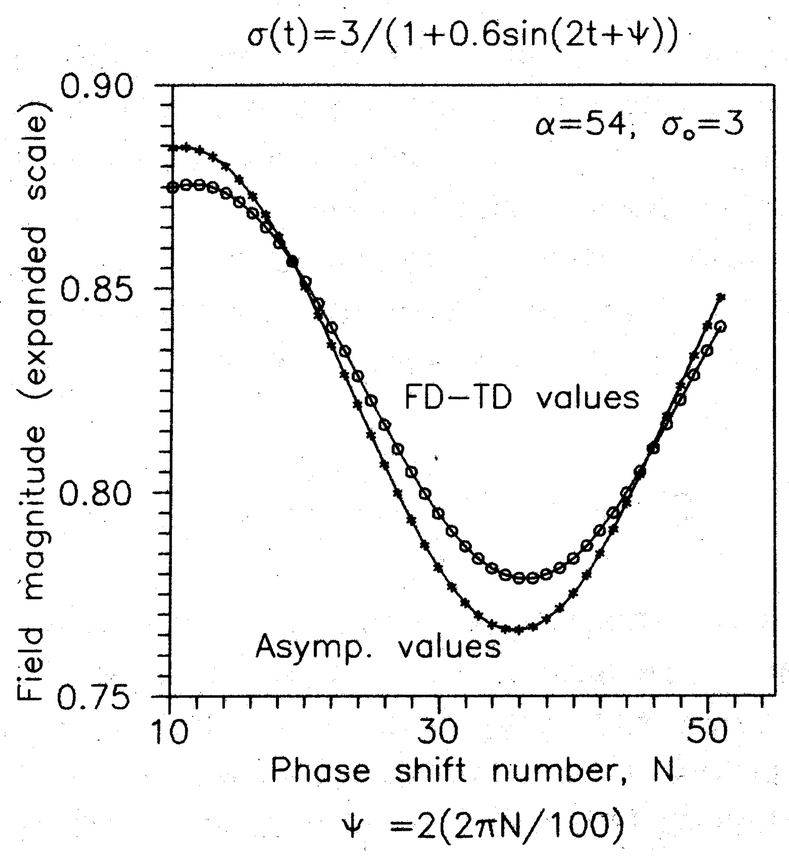

Fig. 3. Reflected field amplitude at illumination frequency versus initial phase shift ψ as obtained both asymptotically and by FDTD for $\nu = 2$, $\sigma_0 = 3$, and $\alpha = 54$.

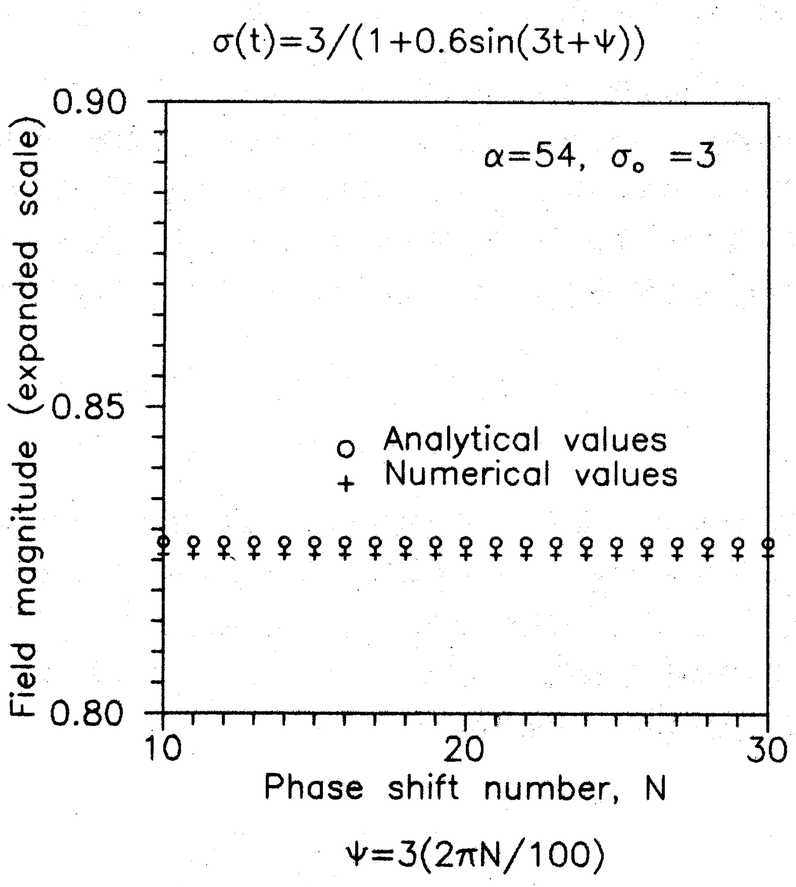

Fig. 4. Reflected field amplitude at illumination frequency versus initial phase as obtained both asymptotically and by FDTD for $\nu = 3$, $\sigma_0 = 3$, and $\alpha = 54$.

To illustrate how these results can be applied to a specific problem, we shall consider the special case where

$$f(t) = \frac{1}{1 + \epsilon \sin(\beta t + \psi)}. \tag{47}$$

For this particular choice of $f(t)$, the variable ξ defined in (32) is given explicitly by

$$\xi = t + \frac{\epsilon}{\beta}(\cos\phi - \cos(\beta t + \psi)). \tag{48}$$

This can be inserted into (41) to determine the c_n. The integrals are reminiscent of Bessel functions and can be numerically integrated. Combining these results with (44) we can deduce the surface value of the scattered field.

Figs. 3 and 4 show the results obtained by both FDTD and the above analysis with $\epsilon = 0.6$ and $\nu = 2$ and 3. The Fourier series summation given by (44) was computed numerically by taking up to 50 terms. The coefficients c_n are computed from integrating (41) using Simpson's rule. We observe again from Fig. 4 the interference effect occurring at only $\nu = 2$.

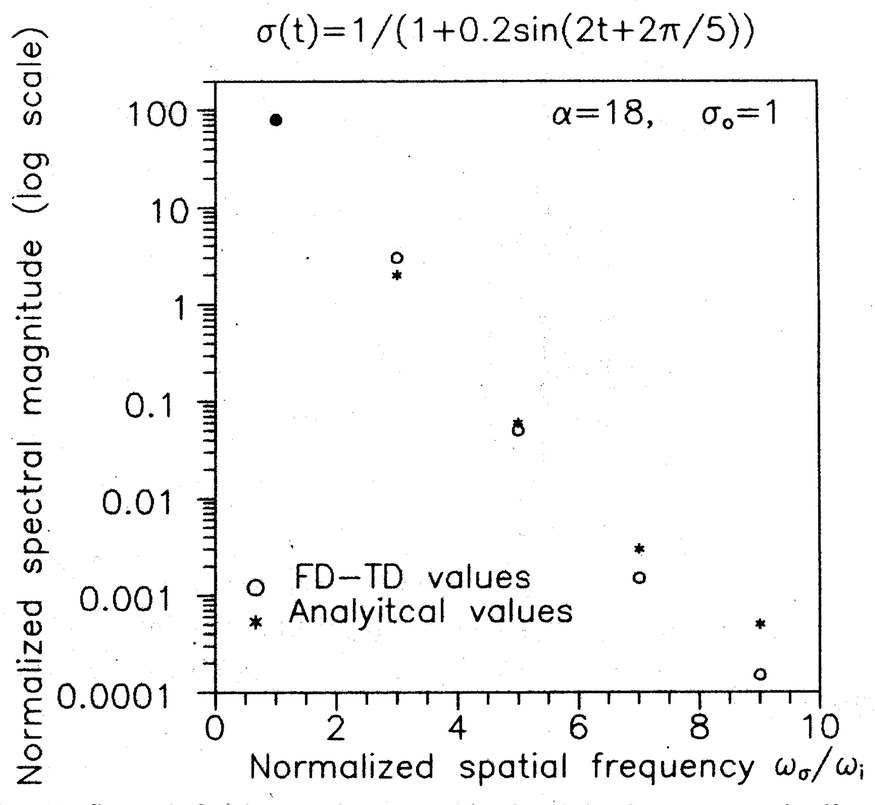

Fig. 5. Reflected field spectrum as obtained both asymptotically and by FDTD for $\nu = 2$, $\sigma_0 = 1$, and $\alpha = 18$.

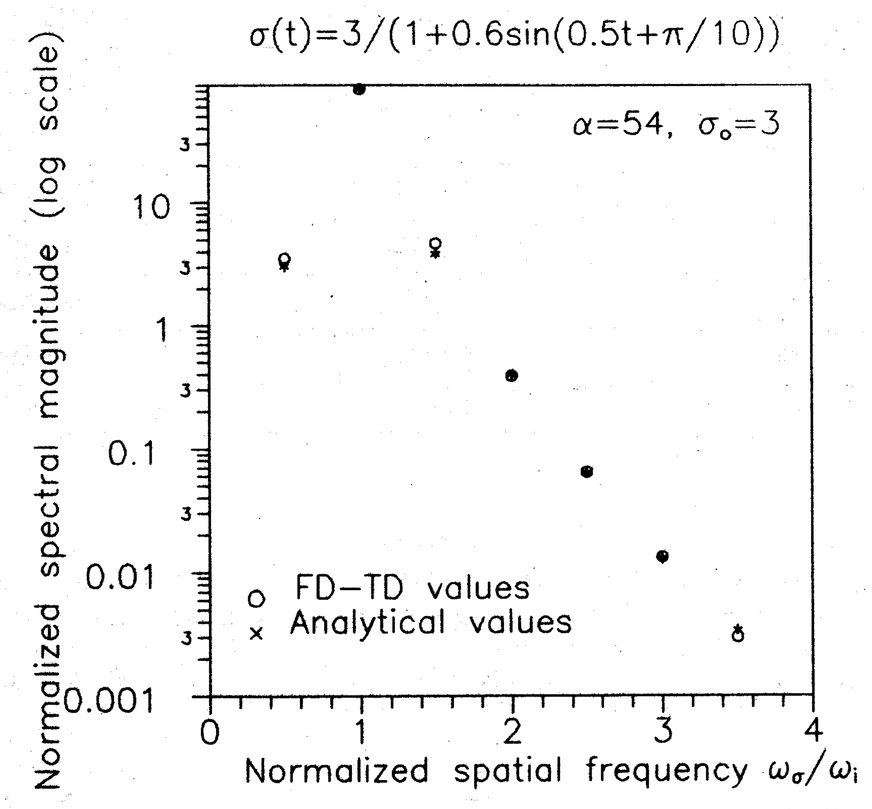

Fig. 6. Reflected field spectrum as obtained both asymptotically and by FDTD for $\nu = 0.5$, $\sigma_0 = 3$, and $\alpha = 54$.

Figs. 5 and 6 compare the scattered field spectrum sidebands as obtained by FDTD and the above analysis for two different values of ν and α. Here, the field magnitude is given in percentage. As α increases, the correspondence between both results improves. This is to be expected for an asymptotic large-α solution.

Tables I–III list the amplitude of the scattered field spectrum sidebands for fixed values of $\alpha = 54$, $\nu = 1$, and three different values of amplitude modulations $\epsilon = 0.2, 0.6, 0.8$. In all cases, a good agreement is shown between the analytical and FDTD numerical results. The degree of agreement is seen to be independent of the choice of ϵ.

B. Deeper Penetration into the Time-Variable Half-Space

Fig. 7 is a schematic diagram of the different boundary layers present in space-time coordinates for our problem. In the previous section, we solved for the field in a thin layer

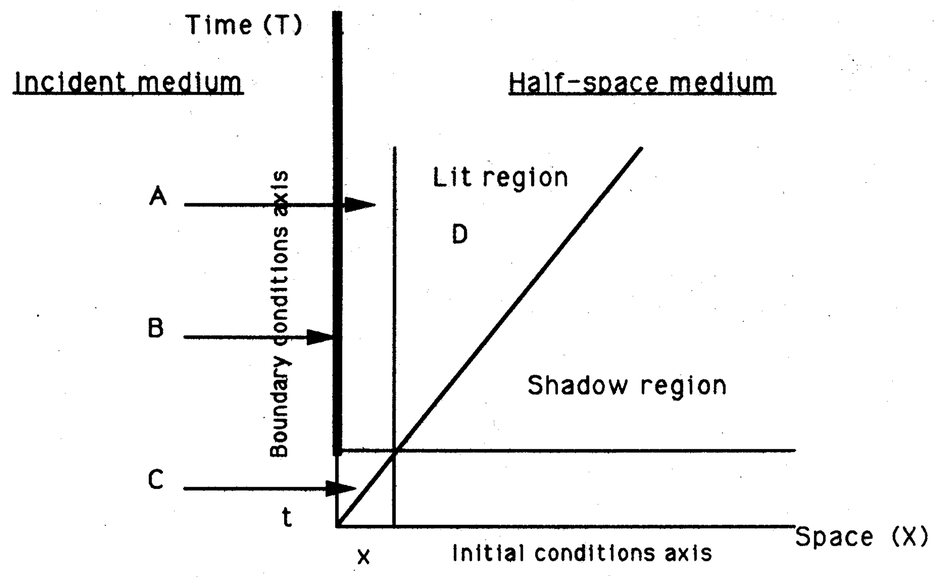

Fig. 7. Boundary-layers in a media with a time-varying conductivity. A: Diffusion solution, B: oscillating solution, C: propagating solution, D: large parameter solution.

TABLE I
FOURIER COMPONENTS OF THE REFLECTED SIGNAL FOR $\epsilon = 0.8$, $\sigma_0 = 3$, $\alpha = 54$ AND $\nu = 1$ AS OBTAINED ANALYTICALLY AND NUMERICALLY

Frequency	Analytical Value	FDTD Value
ω_i	84.772	84.737
$\omega_i + 1\omega_\sigma$	6.3494	7.8026
$\omega_i + 2\omega_\sigma$	0.9818	0.9974
$\omega_i + 3\omega_\sigma$	0.2184	0.2252
$\omega_i + 4\omega_\sigma$	0.0565	0.0626
$\omega_i + 5\omega_\sigma$	0.0162	0.0196
$\omega_i + 6\omega_\sigma$	0.0062	0.0074

TABLE II
FOURIER COMPONENTS OF THE REFLECTED SIGNAL FOR $\epsilon = 0.6$, $\sigma_0 = 3$, $\alpha = 54$ AND $\nu = 1$ AS OBTAINED ANALYTICALLY AND NUMERICALLY

Frequency	Analytical Value	FDTD Value
ω_i	83.951	83.923
$\omega_i + 1\omega_\sigma$	4.2760	5.2934
$\omega_i + 2\omega_\sigma$	0.4478	0.4397
$\omega_i + 3\omega_\sigma$	0.0687	0.0668
$\omega_i + 4\omega_\sigma$	0.0123	0.0126
$\omega_i + 5\omega_\sigma$	0.0257	0.0274

TABLE III
FOURIER COMPONENTS OF THE REFLECTED SIGNAL FOR $\epsilon = 0.2$, $\sigma_0 = 3$, $\alpha = 54$ AND $\nu = 1$ AS OBTAINED ANALYTICALLY AND NUMERICALLY

Frequency	Analytical Value	FDTD Value
ω_i	82.961	83.116
$\omega_i + 1\omega_\sigma$	1.2882	1.6106
$\omega_i + 2\omega_\sigma$	0.0421	0.0401
$\omega_i + 3\omega_\sigma$	0.0197	0.0191
$\omega_i + 4\omega_\sigma$	0.0002	0.0001

around $x \approx 0$. This is represented in Fig. 7 by the region labeled as A. Here the form of solution is diffusive. Enclosed in region A is the boundary region, labeled B, where the solution is oscillating in time. Still, both regions A and B do not result in a propagating solution. But, a propagating solution in the conductive region is seen to originate from region C next to the space time origin where the solution form in regions A and B are not valid. In this section, we shall seek a solution for the fields in region D, away from the thin layer, where $x > 0$. Later, in Section V, we will match the solution forms in regions C and D.

To obtain an accurate approximation of the exponentially small fields in this region, we employ an analysis similar to that found in geometrical optics. We assume that the field is of the form

$$\Omega = e^{-\alpha\psi(x,t)}\left[A(x,t) + O\left(\frac{1}{\alpha}\right)\right]. \tag{49}$$

As $\alpha \to \infty$. This representation is formally valid except in boundary layers and near caustics, if they exist. We note here the similarity with a ray analysis or high-frequency method, where instead of the wavenumber k, we now have α.

Substituting (49) into (1) and equating coefficients of like powers of α, we obtain to two orders in α

$$\psi_x^2 - \psi_t^2 + \psi_t f = 0 \tag{50}$$

$$2A_x\psi_x + A\psi_{xx} - 2A_t\psi_t + A\psi_{tt} - (Af)_t = 0 \tag{51}$$

which are the analogs of the eikonal and transport equations respectively. Equation (50) is a nonlinear first-order partial differential equation, with a time-varying coefficient which can be solved by the method of characteristics [10], [11]. Accordingly we begin by defining the following variables:

$$p = \psi_x(x,t); \qquad q = \psi_t(x,t) \tag{52}$$

$$H(p,q,t) = p^2 - q^2 + qf = 0. \tag{53}$$

We now introduce a family of curves called characteristics (the analogs of rays) which are everywhere orthogonal to the surface defined by H = constant. Denoting by τ the parameter which parameterizes a curve, i.e., $x = x(\tau)$ and $t = t(\tau)$, the orthogonality condition leads to

$$\frac{dx}{d\tau} = \frac{\partial H}{\partial p} = 2p \tag{54}$$

$$\frac{dt}{d\tau} = \frac{\partial H}{\partial q} = f - 2q. \tag{55}$$

From these equations we obtain

$$\frac{d\psi}{d\tau} = -qf. \tag{56}$$

It can also be shown that [10], [11]

$$\frac{dp}{d\tau} = 0 \tag{57}$$

$$\frac{dq}{d\tau} = -\frac{\partial H}{\partial t} = -qf_t, \tag{58}$$

because H does not depend explicitly upon ψ.

The data needed to solve the initial-value problem (54)–(58) requires knowledge of x, q, p and ψ along a curve which is not a characteristic, in the $x - t$ plane. For the given problem, the curve degenerates into a point, the origin, as this is the "source" of the field (see Section V). The characteristics emanating from the origin are labeled by

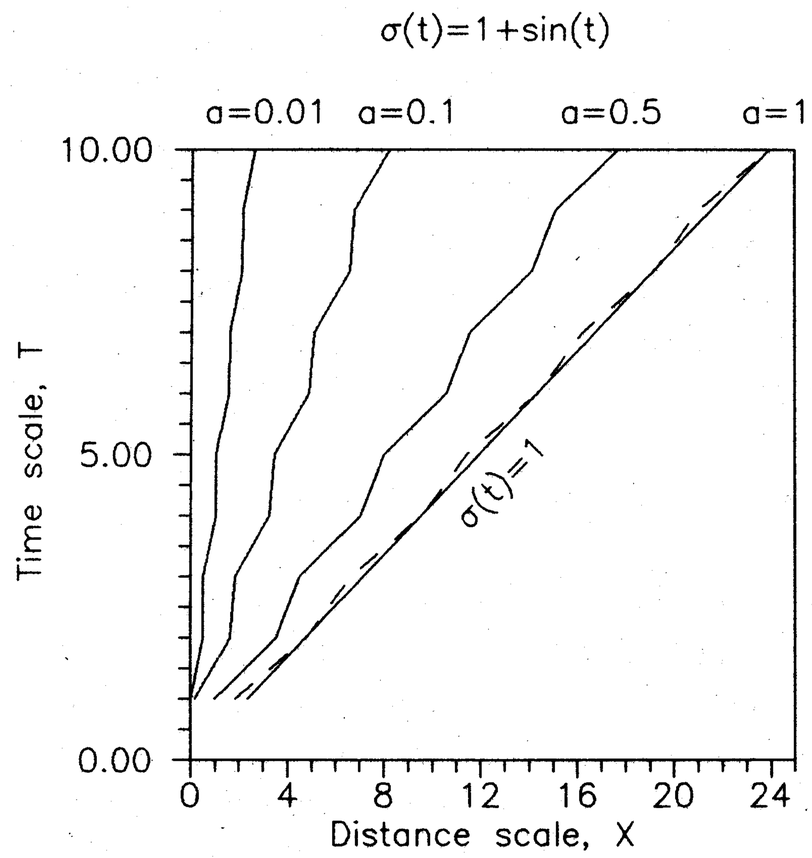

Fig. 8. Rays tracing in (x, t) space for a given time-modulated conductivity and different firing angles.

$p(0) = p_0$, as p remains a constant by (57) along each curve. The values of $x(0)$ and $t(0)$ are both zero and $q(0)$ is determined from (53). If we write

$$p_0 = \frac{f(0)}{2} \sinh \theta \tag{59}$$

then $q(0)$ is given by (53) as

$$q(0) = q_0 = \pm \frac{\cosh \theta}{\sinh \theta}. \tag{60}$$

Finally, the value of $\psi(0)$ is unknown at this stage and will be determined in Section V. Solving the equation $H = 0$ for q, inserting this expression into (55) and noting that $p = p_0$ we obtain

$$\tau(t) = \int_0^t \frac{ds}{\sqrt{f^2(s) + 4p_0^2}}. \tag{61}$$

Combining (55), (59), (61) and the fact that $p = p_0$, we find that x is given by

$$x(t) = f(0) \sinh \theta \int_0^t \frac{ds}{\sqrt{f^2(s) + f^2(0) \sinh^2 \theta}} \tag{62}$$

where θ is now the new label of a ray. We now have a formula for the characteristics (or rays) in the space time coordinates given by the integral solution for x(t).

Fig. 8 shows several characteristics for different values of θ where $a = f(0) \sinh(\theta)$. Therefore each variable a in Fig. 8 represents a particular angle θ referred to as firing angle. All the curves are confined to the region $t > x$, showing that the solution is causal. For vertically launched rays ($\theta \to 0$), the modulation is less apparent and the ray acts more like a straight line. Moreover, this region is devoid of any geometric singularity such as caustics (bending rays) or foci (intersecting rays). Finally, we observe that (56) can be integrated in principle to determine the phase, yielding

$$\psi = \psi(0) - \int_0^\tau q(\tau') f(t(\tau'))\, d\tau'. \tag{63}$$

By introducing τ and θ as new independent variables in (51), we find that A satisfies

$$A_\tau + \left(\frac{J_\tau}{2J} + \frac{f_t}{2}\right) A = 0 \tag{64}$$

where J is the Jacobian given by

$$x_\tau t_\theta - x_\theta t_\tau. \tag{65}$$

The solution of (64) is

$$A(\tau) = \frac{C(\theta)}{\sqrt{J}} e^{-\int_0^\tau \frac{f_t}{2} d\tau'}. \tag{66}$$

We observe that the Jacobian vanishes at the origin, so that (49) is invalid there. The local analysis required to remove this nonuniformity is presented in the next section. The constant $C(\theta)$ will be computed there.

V. Matching of the Asymptotic and Boundary Layer Solutions

We shall first illustrate how the results obtained in the previous section are applied by considering the case of a fixed half-space conductivity σ_0. Under such circumstances, it is found that

$$J(x, t) = -\frac{2(t^2 - x^2)}{t} \tag{67}$$

$$\psi(x, t) = -\frac{\sigma_0}{2}\left(\sqrt{t^2 - x^2} - t\right). \tag{68}$$

This leads to

$$\Omega(x, t) = \frac{C\sqrt{t}}{\sqrt{2(t^2 - x^2)}} e^{-\alpha \frac{\sigma_0}{2}\left(t - \sqrt{t^2 - x^2}\right)}. \tag{69}$$

The line $x = t$ defines a caustic, or more precisely, the boundary of the Fresnel region that separates the "lit" region from the "shadow" region. The solution given by (69) reduces to the diffusion solution obtained earlier, as we approach the thin boundary layer strip at $x = 0$. A matching of the results of (36) and (69) leads to

$$C = -4\sqrt{\frac{2}{\pi}} \frac{h(0)}{\alpha^{3/2}} \left(\frac{t}{x}\right)^2. \tag{70}$$

This matching procedure is based on the assumption that the regions where (36) and (69) are valid overlap. Matching is performed by comparing the asymptotic expansion of (69) as $x \to 0$ with the solution of (36) as $\bar{x} \to \infty$. It is noted that C is a function of x/t. This is an expected result because for small x, $p_0 \approx x\sigma_0/2t$ so $C(p_0)$ becomes $C(x/t)$. The field description around the origin can be found with the change of variables $x \to \alpha x$ and $t \to \alpha t$. By retaining terms of order α^2, we obtain

$$\Omega_{xx} = \Omega_{tt} + \sigma_0 \Omega_t. \tag{71}$$

Using the Laplace transform and a contour integral around the branch cuts, it can be shown that the steady-state response

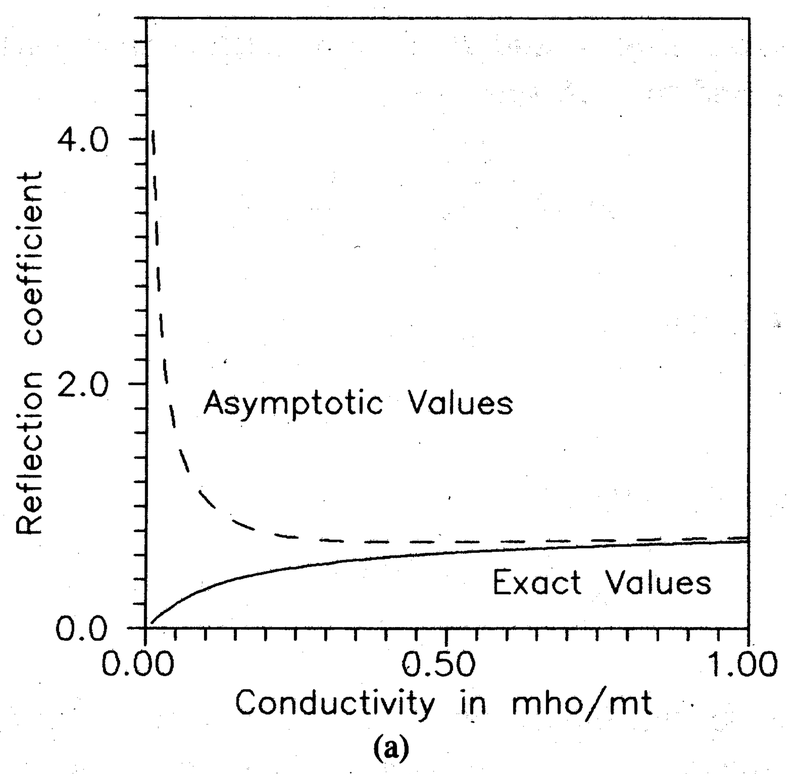

(a)

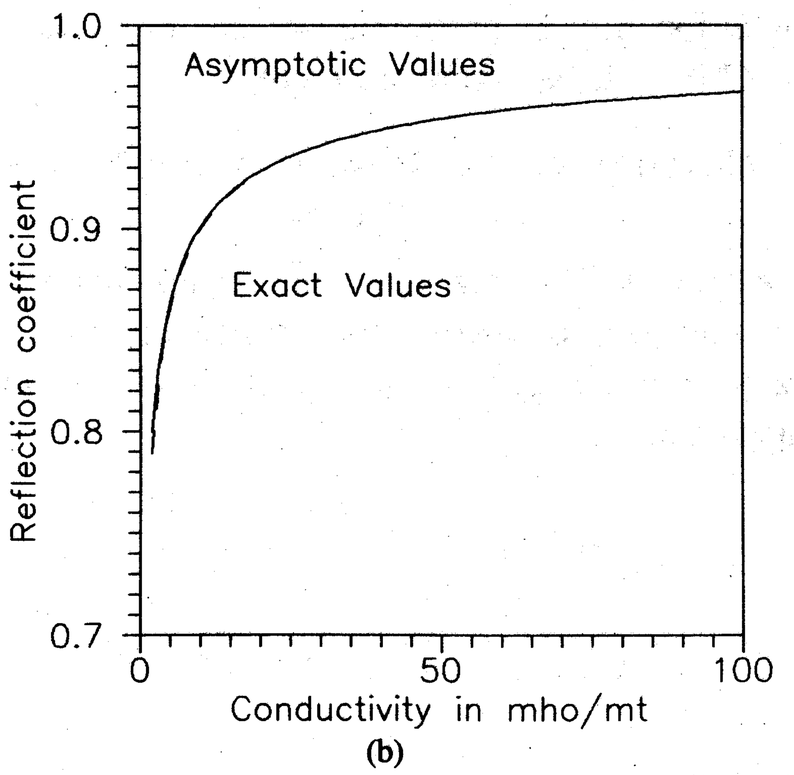

(b)

Fig. 9. Variations of the reflected field amplitude versus fixed conductivity σ_0 as obtained both exactly and asymptotically.

is given by

$$-\operatorname{Im}\frac{2e^{-i\sqrt{i\alpha}x}e^{-it}}{\sqrt{\alpha}\,e^{i\frac{\pi}{4}}}. \tag{72}$$

At $x = 0$ the above equation can be written as

$$\Omega(0, t) = \frac{2}{\sqrt{\alpha}}\sin\left(t + \frac{\pi}{4}\right). \tag{73}$$

This corresponds exactly to the solution that would be obtained by using (44) and (46) with a fixed conductivity. To have an idea on the range of α satisfying the definition of "large" the reflected field magnitude is calculated using the asymptotic solution (46) for fixed conductivity and rewritten as

$$U^{sc}(0, t) = \sqrt{\frac{2}{\alpha - 1}}\sin t + \sqrt{\frac{2}{\alpha}}\cos t. \tag{74}$$

The amplitude of the reflected field is defined as the square root of the sum of the square coefficients multiplying the sin and cos terms. This latter is compared against the exact formula of the reflection coefficient given as

$$\rho = \left|\frac{1 - \sqrt{j\alpha - 1}}{1 + \sqrt{j\alpha + 1}}\right|. \tag{75}$$

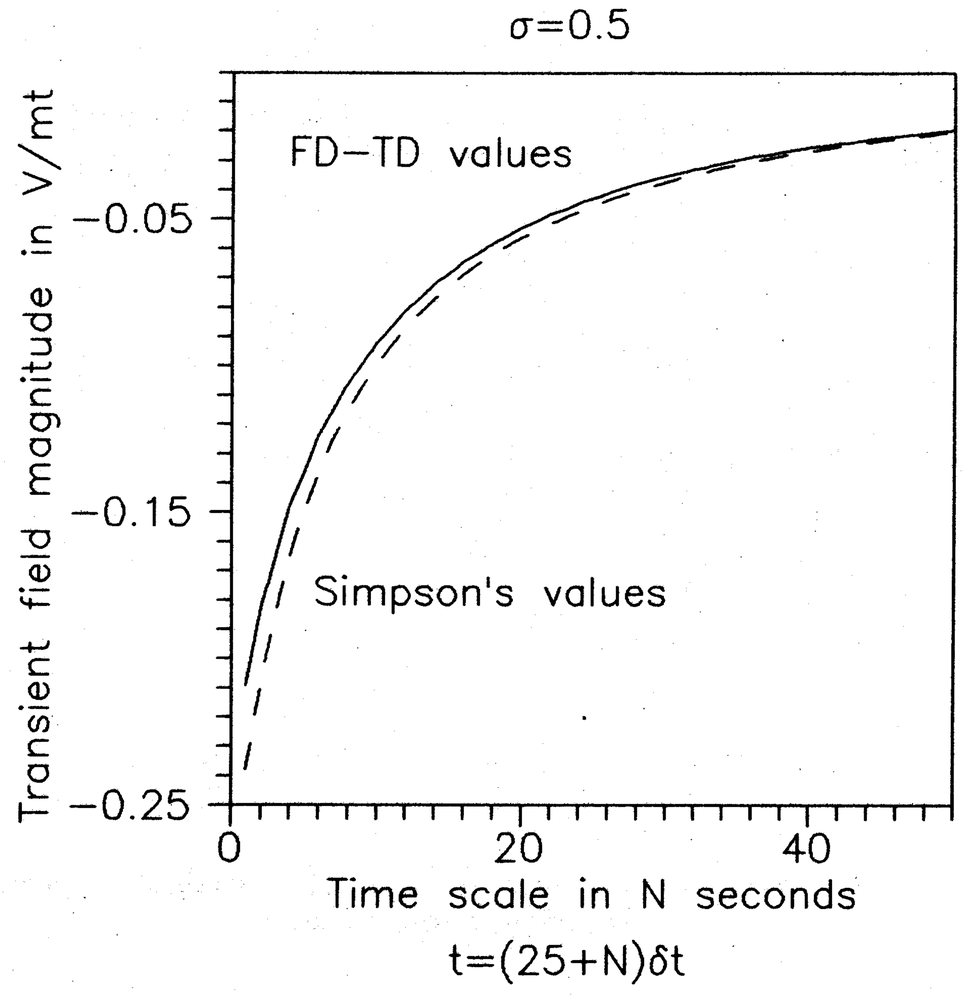

Fig. 10. Transient response in the reflected field from a material with a constant conductivity σ_0 as obtained by numerical integration and FDTD.

Results are plotted in Fig. 9. The transient response is given by the integral

$$T = -2\frac{\alpha}{\pi}\int_0^1 \frac{e^{-\alpha v t}}{1 + \alpha^2 v^2} \cdot\left[-v\sin(\alpha\beta x) + \beta\cos(\alpha\beta x)\right] dv \tag{76}$$

where $\beta = \sqrt{v - v^2}$. Equation (76) reduces to (11) for $x = 0$. This integral can be evaluated numerically and compared against the FDTD results. Such a comparison for $x = 0$ is shown in Fig. 10. For a fixed $\bar{x}$ and t, it can be shown the results given by (72) and (76) reduce to the result derived from (36) as $\alpha \to \infty$. It can also be shown that by fixing (x, t) and letting $\alpha \to \infty$, these results converge to the geometrical optics result given by (69). The resulting expression for C obtained by matching both results along a ray defined by $t = mx$, where m is large, reduces to the same expression for C defined in (70).

It has been shown the results obtained so far are valid for the constant-conductivity case. We shall now reconsider the case of a time-varying conductivity. The results describing our amplitude and phase functions are, in general, impossible to solve exactly because of the difficulty in solving for τ and p_0 in terms of x and t. However, we can consider limiting cases. Our interest is in finding a solution in the narrow strip next to the boundary. As $p_0 \to 0$ it can be shown that

$$\psi(\xi) = \frac{x^2}{4\xi} \tag{77}$$

$$A(\xi) = \frac{C(p_0)}{\sqrt{2\xi}\,f(\xi)} \tag{78}$$

where again

$$\xi = \int_0^t \frac{d\tau}{f(\tau)}. \tag{79}$$

Therefore,

$$\Omega(x,\xi) = \frac{C(p_0)}{\sqrt{2\xi}\, f(\xi)}\, e^{-\frac{\alpha\tau^2}{4\xi}}. \tag{80}$$

A matching of (80) with (36) leads to

$$C(p_0) = -\frac{4\sqrt{2}}{\alpha^{3/2}\sqrt{\pi}}\, h(0)\left(\frac{\xi}{x}\right)^2 \tag{81}$$

which is similar in form to (70). The next limiting case is when $\tau \to 0$. This case leads to results similar to the fixed-conductivity case, where σ_0 in (69) is replaced by $f(0)$, and where $f(t)$ behaves like $f(0)$ next to the origin where $t = 0$.

VI. Summary and Conclusion

We have presented in this paper a detailed analysis of electromagnetic wave interactions with a material half-space having time-varying conductivity. At each stage, the results were verified by considering limiting cases. We also performed a matching of the different solution regions. Three different analysis methods were utilized: a simple first-order regular perturbation method; a large-parameter asymptotic analysis; and a large-parameter analysis similar to geometrical optics. A purely numerical FDTD code was used to obtain comparative results. Numerical and analytical results for the two types of conductivity variations considered were found to be in good agreement.

Our results indicate the presence of sidebands in the scattered field spectrum and an interference effect occurring when the material conductivity varies at twice the illuminating frequency. The characteristics inside the half-space are modulated as they propagate inside the material, and are seen to emanate from the origin in the $x - t$ coordinate system. No intersection of rays (focusing effect) is detected. With the introduction of boundary layers, it becomes clear how the propagating and nonpropagating dissipative solutions are generated inside a conductive material.

Finally, the FDTD method has been shown to provide in a straightforward manner numerical predictions for scattering by the time-varying half-space that closely agree with the data obtained from the detailed analysis. We note that the FDTD model is restricted to the limiting cases of material conductivity variation required to make the detailed analysis tractable. Therefore, extension of the FDTD numerical model of time-varying media to two dimensions appears to be feasible. This would permit simulation of compact material targets having time-varying volumetric or surface constitutive parameters generating unusual electromagnetic phenomena. It may be possible to exploit these phenomena for engineering to achieve real-time control of target radiation and scattering properties.

References

[1] D. E. Holdberg and K. S. Kunz, "Parametric properties of fields in a slab of time-varying permittivity," *IEEE Trans. Antennas Propagat.*, vol. AP-14, pp. 183–194, Mar. 1966.

[2] R. L. Fante, "On the propagation of electromagnetic waves through a time-varying dielectric layer," *Appl. Sci. Res.*, vol. 27, pp. 341–354, Apr. 1973.

[3] ____, "Optical propagation in space-time media using many-space-scale perturbation theory," *J. Opt. Soc. Am.*, vol. 62, pp. 1052–1060, Sept. 1972.

[4] F. R. Morgenthaler, "Velocity modulation of electromagnetic waves," *IRE Trans. Microwave Theory Tech.*, vol. MTT-6, pp. 167–172, Apr. 1958.

[5] A. Hessel and A. A. Oliner, "Wave propagation in a medium with a progressive sinusoidal disturbance," *IRE Trans. Microwave Theory Tech.*, vol. MTT-9, pp. 337–339, July 1961.

[6] J. C. Simon, "Action of a progressive disturbance on a guided electromagnetic wave," *IRE Trans. Microwave Theory Tech.*, vol. MTT-14, pp. 18–22, Jan. 1966.

[7] A. Taflove, "Review of the formulation and applications of the finite-difference time-domain method for numerical modeling of electromagnetic wave interactions with arbitrary structures," *Wave Motion*, vol. 10, Dec. 1988.

[8] J. K. Cohen and R. M. Lewis, "A ray method for the asymptotic solution of the diffusion equation," *J. Inst. Math. Appl.* no. 3, pp. 266–290, 1967.

[9] H. S. Carslaw and J. C. Jaeger, *Conduction of Heat in Solids.* Oxford: Clarendon, 1959.

[10] N. Bleistein, *Mathematical Methods for Wave Phenomena.* New York: Academic, 1984.

[11] J. Fritz, *Partial Differential Equations.* New York: Springer-Verlag, 1978.

[12] F. Harfoush, "Analysis and numerical modeling of electromagnetic waves scattering from time varying surfaces in one and two dimensions," Ph.D. dissertation, Northwestern Univ., Evanston, IL, Aug. 1988.

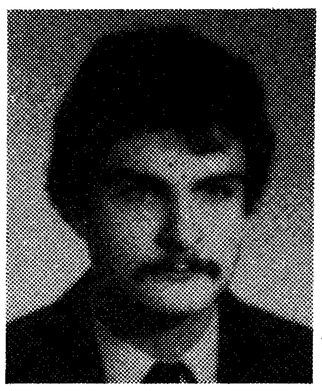

Fady A. Harfoush (S'85–M'87–S'87–M'88) was born in Beirut, Lebanon, on January 16, 1957. He received the B.S. degree in electrical engineering from Boğaziçi University, Istanbul, Turkey, in 1981, and the M.S. and Ph.D. degrees in electrical engineering from Northwestern University, Evanston, IL, in 1984 and 1988, respectively.

From 1984 to 1988, while at Northwestern, he worked on the scattering and penetration of electromagnetic waves using both the finite difference time domain technique and analytical methods. In 1988 he joined the Fermi National Accelerator Laboratory, Batavia, IL, where his research activities include the area of computational electromagnetics for the modeling of static and time dependent electromagnetic problems in accelerator physics.

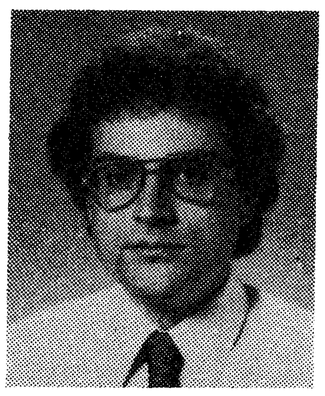

Allen Taflove (M'75–SM'84–F'90) was born in Chicago, IL, on June 14, 1949. He received the B.S. (with highest distinction), M.S., and Ph.D. degrees in electrical engineering from Northwestern University, Evanston, IL, in 1971, 1972, and 1975, respectively.

From 1975 to 1984, he was a staff member in the Electronics Division, IIT Research Institute, Chicago, IL, holding the positions of Associate Engineer, Research Engineer, and Senior Engineer. During this time, he was principal investigator on a number of externally funded research programs, including five that contributed to the early development of the finite-difference time-domain method for computational modeling of electromagnetic wave interactions with complex structures. He was also a key contributor to large-scale programs involving the application of radio-frequency heating to produce oil in place (without mining) from deposits of oil shale, tar sands, and heavy oil; to accelerate oil production from slowly producing conventional wells; and to decontaminate large sections of the ground permeated with toxic chemical wastes. In this technical area, he has been awarded 10 U.S. patents to date. In 1984, he returned to Northwestern University where he is currently Professor of Electrical Engineering and Computer Science. He is actively pursuing supercomputing computational electromagnetics modeling of a broad variety of phenomena and technologies, including radiation and scattering, high-speed digital electronics, microwave/millimeter wave circuits, and optical pulse propagation and switching. He also co-originated and is active in Northwestern's innovative Honors Program in Undergraduate Research, wherein extremely bright high school graduates participate in an accelerated, research-enriched curriculum leading to the Ph.D. in as little as six years.

Dr. Taflove is a member of Tau Beta Pi, Eta Kappa Nu, Sigma Xi, Commission B of URSI, and the Electromagnetics Academy. During 1990–1991, he was a Distinguished National Lecturer for the IEEE Antennas and Propagation Society, and he is Chairman of the Technical Program of the 1992 IEEE Antennas and Propagation Society International Symposium to be held in Chicago. He is co-author of the Best Paper at the 1983 IEEE International EMC Symposium, Washington, DC.